Virology 509 (2017) 195–204

Contents lists available at ScienceDirect

Virology

journal homepage: www.elsevier.com/locate/yviro

Differential replication of Foot-and-mouth disease viruses in mice determine lethality

Marco Cacciabue[a,e,1], María Soledad García-Núñez[a,1], Fernando Delgado[b], Anabella Currá[a,e], Rubén Marrero[a], Paula Molinari[a,e], Elizabeth Rieder[c], Elisa Carrillo[d,e], María Inés Gismondi[a,e,*]

[a] Instituto de Biotecnología, Instituto Nacional de Tecnología Agropecuaria (INTA), De los Reseros y N. Repetto s/n, (1686) Hurlingham, Argentina
[b] Instituto de Patobiología, INTA, De los Reseros y N. Repetto s/n, (1686) Hurlingham, Argentina
[c] Foreign Animal Disease Research Unit, United States Department of Agriculture, Agricultural Research Service, Plum Island Animal Disease Center, PO Box 848, Greenport, NY11944-0848, USA
[d] Centro de Investigación en Ciencias Veterinarias y Agronómicas (CICVyA), INTA, De los Reseros y N. Repetto s/n, (1686) Hurlingham, Argentina
[e] Consejo Nacional de Investigaciones Científicas y Técnicas (CONICET), Argentina

ARTICLE INFO

Keywords:
Pathogenesis
Lethality
FMDV
Adult mice
2C protein
Capsid

ABSTRACT

Adult C57BL/6J mice have been used to study *Foot-and-mouth disease virus* (FMDV) biology. In this work, two variants of an FMDV A/Arg/01 strain exhibiting differential pathogenicity in adult mice were identified and characterized: a non-lethal virus (A01NL) caused mild signs of disease, whereas a lethal virus (A01L) caused death within 24–48 h independently of the dose used. Both viruses caused a systemic infection with pathological changes in the exocrine pancreas. Virus A01L reached higher viral loads in plasma and organs of inoculated mice as well as increased replication in an ovine kidney cell line. Complete consensus sequences revealed 6 non-synonymous changes between A01L and A10NL genomes that might be linked to replication differences, as suggested by *in silico* prediction studies. Our results highlight the biological significance of discrete genomic variations and reinforce the usefulness of this animal model to study viral determinants of lethality.

1. Introduction

Foot-and-mouth disease (FMD) is a highly contagious viral disease of wild and domestic cloven-hoofed animals. The disease has major economic impact due to severe productivity losses and to the restrictions imposed to the trade of animals and animal products from FMD-affected regions (Sobrino, 2004). Prevention and control of FMD is achieved by sanitary profilaxis as well as vaccination of susceptible animals in endemic areas.

The etiological agent of FMD is *Foot-and-mouth disease virus* (FMDV), the prototype member of the genus *Aphthovirus* within the *Picornaviridae* family. The viral particle is an icosahedron which encloses a single-stranded positive-sense RNA of approximately 8200 nucleotides that is linked covalently to the viral protein VPg at its 5′ end. The viral genome is flanked by untranslated regions at both its 5′ and 3′ termini and encodes a polyprotein that is subjected to co-translational cleavage to produce the 4 capsid proteins (VP4, VP2, VP3 and VP1) and 10 non-structural proteins (Lpro, 2A, 2B, 2C, 3A, 3B1, 3B2, 3B3, 3Cpro and 3Dpol) (Grubman and Baxt, 2004). Like other RNA viruses, FMDV replication is catalyzed by an error-prone viral RNA polymerase (3Dpol) and consequently the virus appears as a population of different but phylogenetically-related variants known as the viral quasispecies (Haydon et al., 2001; Domingo et al., 2003, 1980; Sobrino et al., 1983). The virus exists as 7 immunologically different serotypes (A, O, C, Asia, SAT1, SAT2, SAT3) and multiple subtypes that elicit effective neutralizing antibodies that do not confer cross-protection among serotypes.

Natural FMDV infection in cattle occurs mainly *via* the respiratory route by aerosolized virus and subsequent primary infection of nasopharynx and lung, followed by a viremic phase and dissemination to secondary replication sites (reviewed by Arzt et al., 2011). Although many aspects of FMD in natural hosts have been studied extensively, viral and host factors related to FMDV virulence and pathogenesis are not completely understood. It is well known that FMDV leader proteinase (Lpro) plays a role as a virulence factor, since viruses of serotype A lacking this region or carrying mutations within Lpro

* Correspondence to: Instituto de Biotecnología, Instituto Nacional de Tecnología Agropecuaria, De los Reseros y N. Repetto, 1686 Hurlingham, Buenos Aires, Argentina.
E-mail addresses: cacciabue.marco@inta.gob.ar (M. Cacciabue), solegarnu@yahoo.com (M.S. García-Nuñez), delgado.fernando@inta.gob.ar (F. Delgado), curra.anabella@inta.gob.ar (A. Currá), marrerodiaz.ruben@inta.gob.ar (R. Marrero), Molinari.maria@inta.gob.ar (P. Molinari), elizabeth.rieder@ars.usda.gov (E. Rieder), carrillo.elisa@inta.gob.ar (E. Carrillo), gismondi.maria@inta.gob.ar (M.I. Gismondi).
[1] These authors contributed equally to this work.

http://dx.doi.org/10.1016/j.virol.2017.06.012
Received 1 February 2017; Received in revised form 1 June 2017; Accepted 12 June 2017
Available online 23 June 2017
0042-6822/ © 2017 Elsevier Inc. All rights reserved.

display an attenuated phenotype in cell culture and show no replication in cattle and pigs (Chinsangaram et al., 1998; Mason et al., 1997; Díaz-San Segundo et al., 2012). Other viral proteins such as 3A or structural proteins have also been proposed as virulence determinants both in cell culture and in natural hosts. Indeed, Pacheco et al. demonstrated that 3A protein of type O1Campos is relevant for replication in cattle and in primary cell cultures of bovine origin (Pacheco et al., 2013), and this viral protein has also been associated with FMDV adaptation to the guinea pig (Núñez et al., 2001). Other authors have shown that VP1, VP2 and VP3 proteins are determinants of FMDV pathogenesis in cattle and swine (Lohse et al., 2012; Bøtner et al., 2011), and deletions of the RGD motif in VP1 (Rieder et al., 1996) or acquisition of positive charge have been related to attenuation in cattle and swine (Borca et al., 2012; Sa-Carvalho et al., 1997; Zhao et al., 2003; Lawrence et al., 2016a, 2016b).

The study of FMDV virulence factors in natural hosts has a major limitation related to the logistics and cost of experimentation with large animals. To overcome this difficulty, several laboratory animal models have been developed that may be useful to study particular aspects of FMD pathogenesis and FMDV biology (Habiela et al., 2014; Skinner, 1951; Waldman and Pape, 1920). In particular, after footpad subcutaneous (sc) injection or intraperitoneal (ip) inoculation the virus causes an acute infection that can be lethal in adult C57BL/6 mice. Subcutaneous injection produces a systemic infection with viral dissemination to different organs (heart, lung, brain, kidney, liver, spleen, pancreas, and thymus) that leads to death of animals at 48–72 hpi. Finally, the disease is associated with a pronounced lymphopenia and depletion of splenic $CD4^+$ and $CD8^+$ T-lymphocytes (Salguero et al., 2005).

Interestingly, C57BL/6 mice proved to be adequate to detect virulence differences among FMDV variants of the same serotype and thus this animal model appears as a powerful tool to study viral factors related to virulence and/or pathogenesis (Salguero et al., 2005). In fact, in a study on the virulence of field strains that circulated in Argentina during the 2000–2002 epizootic, we demonstrated previously that FMDV A/Arg/00, as opposed to FMDV A/Arg/01, does not cause death of C57BL/6 mice when inoculated ip even at doses as high as 10^7 pfu per animal; these observations mirrored the pathogenic behavior of field strains (García Núñez et al., 2010; Mattion et al., 2004).

In this work, we further characterize two FMDV A/Arg/01 variants in terms of pathogenicity in adult mice and replication in cell culture.

2. Material and methods

2.1. Viruses and cell lines

A01NL and A01L viruses were obtained from the National Institute for Animal Health (SENASA, Argentina). Viruses were isolated during the FMDV outbreak that occurred in Argentina during years 2000–2001 and belong to serotype A/Arg/01. All experiments were conducted using fourth cell passages of each FMDV in baby hamster kidney cells (BHK-21 clone 13; ATCC CCL10). Quantification of viral particles present in various samples were determined in BHK-21 cells by plaque assay (pfu/ml) or alternatively the 50% tissue culture infective dose ($TCID_{50}$) was calculated by the end point dilution method using the formula of Reed and Muench (Reed and Muench, 1938).

Cell lines used in this study were BHK-21, PK15-C1 (ATCC, PTA-8244), IBRS-2, MDBK (ATCC CCL22), fetal bovine kidney cells (FBK) and ovine kidney cells (OK) (Zabal and Fondevila, 2013). Cells were maintained at 37 °C and 5% CO_2 in Dulbecco's modified Eagle´s medium (DMEM, Life Technologies, Grand Island, NY, USA) supplemented with 10% fetal bovine serum (FBS) and antibiotics (Gibco-BRL/Invitrogen, Carlsbad, CA, USA).

2.2. Mice

Eight to 10-week-old female C57BL/6J/LAE mice were purchased from University of La Plata, Argentina. Mice were maintained under specific pathogen-free conditions and allowed to acclimatize to the biosafety level 4 OIE (BSL-4 OIE) animal facility at the Institute of Virology, INTA, for 1 week prior to experiments.

Experiments with mice were performed in accordance with the Institutional Committee for the Use and Care of Experimentation Animals (CICUAE-INTA protocols Nos. 46/2013 and 49/2015).

2.3. Animal infection and processing of samples

Groups of mice were inoculated with A01L or A01NL by ip injection with 100 microliters of a viral suspension containing the indicated amount of each virus. Mice were examined for clinical symptoms twice daily. Animals were euthanized at a humane endpoint when showing irreversible signs of pain or disease (hypothermia, hunched posture, lethargy).

At different times post inoculation, mice (n=4 per experimental group) were euthanized and organs (liver, spleen, pancreas, thymus, lung, heart and brain) were harvested and weighed. Half of the tissues was used for histological analysis. The other half was mechanically disrupted and resuspended in DMEM supplemented with HEPES 25 mM pH 7.4; cell suspensions were frozen at −80 °C. Lung and heart samples were used exclusively for histological analysis. Whole blood samples were collected in heparinized tubes at different times post-inoculation. Plasma was separated by centrifugation, aliquoted and stored at −80 °C.

For cross-protection experiments, groups of mice (n=5) were inoculated ip with A01NL (10^5 PFU per animal) or DMEM. Fourteen days after first inoculation, mice were bled to determine neutralizing antibody titers and immediately inoculated ip with a lethal dose of A01L virus (10^4 PFU per animal) (Molinari et al., 2010). Mice were bled 24 h post-A01L infection and heparin-anticoagulated plasma samples were stored at −80 °C for quantification of viremia. Animals showing irreversible signs of disease at 24 h post-A01L inoculation were sacrificed to avoid suffering. Surviving mice were examined for clinical symptoms daily for 7 additional days.

2.4. Histopathology

Samples from different organs were fixed in 10% buffered formalin (pH 7.2) for histopathological studies. After fixation, samples were dehydrated through a graded series of alcohol to xylol and embedded in paraffin. Three micrometer-thick sections were cut and stained with hematoxylin and eosin (H & E). Histological grading was made blindly by an experimented pathologist.

2.5. Quantification of neutralizing antibodies

Anti-FMDV neutralizing antibodies were measured by the variable serum-constant virus method as described by Quattrocchi et al. (2011). Briefly, heat-inactivated sera were serially diluted and dilutions were incubated with 100 $TCID_{50}$/well of infectious FMDV for 40 min at 37 °C. The virus-serum mixtures were transferred onto BHK-21 cell monolayers and cytopathic effect was recorded after 48 h incubation at 37 °C in a 5% CO_2 containing atmosphere. Titer of neutralizing antibodies was calculated as log (1/last serum dilution that neutralizes 50% of wells).

2.6. Quantification of IFN-α

Interferon alpha was quantitated (pg/ml) in plasma samples with Mouse IFN alpha Platinum ELISA kit (eBioscience, Vienna, Austria).

2.7. Plaque assays and viral growth curves

Plaque assays were performed as previously described (García Núñez et al., 2010). Monolayers of OK cells were fixed and stained at 24 hpi and the plaques were counted. The values calculated for the number of plaque forming units per milliliter (PFU/ml) were plotted in a logarithmic scale using GraphPad Prism 5.00 (GraphPad Software, San Diego, CA, USA). All assays were performed in duplicate. For viral plaque size determination, 40–60 plaques of each virus were measured with ImageJ 1.42q software (NIH, USA) (Schneider et al., 2012).

For multiple step-growth studies, cells were infected for 30 min at a multiplicity of infection (moi) of 0.1 and washed with PBS pH 5.6 on ice to inactivate unabsorbed virus. After restitution of physiological pH, cells were incubated at 37 °C in a 5% CO_2 atmosphere. At indicated times post-infection, cells were lysed by three consecutive freeze-thaw cycles and the amount of viral particles was measured by the $TCID_{50}$ method as mentioned above.

2.8. Determination of viral sequences

To obtain the complete consensus sequences of A01NL and A01L, viral RNAs were isolated from supernatants of infected cells (fourth passage) or from spleen tissue of inoculated animals obtained at 22 hpi using Trizol reagent (Life Technologies, Carlsbad, CA, USA) according to the manufacturer's instructions. Complementary DNA (cDNA) was synthesized with Superscript III reverse transcriptase (Life Technologies, Carlsbad, CA, USA) as previously described (García Núñez et al., 2014). Oligonucleotides covering the whole FMDV-A genome (Mattion et al., 2004) were used to obtain the complete sequence of both FMDV variants by automated sequencing. GenBank accession numbers of A01L and A01NL consensus sequences are KY404934 and KY404935, respectively.

2.9. In silico modelling and sequence analysis

Amino acid sequences of A01L and A01NL capsid proteins were aligned and their secondary structure was predicted using Chimera software (Pettersen et al., 2004). The structure of each viral protein (VP1, 2, 3, 4) was modelled at the SWISS-MODEL Workspace (Arnold et al., 2006) (homology method without refinement), emergent models were assembled *in silico* into capsomers by structural alignment with a serotype A FMDV template capsomer (PDB accession 1ZBE; Chimera software). Finally, the model of each whole viral particle was assembled at the Virus Particle Explorer (VIPERdb) server (Carrillo-Tripp et al., 2009). Interactions between amino acids from the same or from different capsomers were simulated through a structure-based analysis using VIPERdb.

The electrostatic charge of the capsomers at the 2x axis was calculated using PROPKA software (McGuffin et al., 2015). This program analyzes de protonation state of titratable groups within the structure and predicts their pKa at different pH values.

The identification of titratable groups within the interpentamer 2x axis and prediction of their pKa values at pH 6, 6.5 and 7 was accomplished using PROPKA server. A solvent-excluded molecular surface of each capsomer was created with Chimera embedded software from the MSMS package (Altschul et al., 1997) and subjected to Coulombic Surface Coloring.

The structure of 2C protein for the A01L virus was modelled at the Integrated Protein Structure and Function Prediction Server (McGuffin et al., 2015); besides, 2C proteins of all FMDV serotypes (500 sequences) were retrieved from the BlastP web service (Altschul et al., 1997) and aligned with the Cobalt align tool (Papadopoulos and Agarwala, 2007). The obtained 2C multiple sequence aligment was used as input for the determination of evolutionary conservation scores of amino acids and their projection on protein 2C structure (Landau et al., 2005; Glaser et al., 2003). Finally, multiple sequence alignments of 2C protein of all FMDV serotypes were used to obtain sequence logos (Schneider and Stephens, 1990; Crooks et al., 2004).

2.10. Statistical analysis

Student's *t*-test was used to compare mean viral titers in different samples and mean plaque diameters. A p value < 0.05 was considered as statistically significant.

3. Results

3.1. Pathogenicity of FMDV A/Arg/01 variants

During the FMDV epizootic that occurred in years 2000–2002 in Argentina, circulation of a virulent strain causing severe lesions in affected animals and leading to death of calves in the field was reported (Mattion et al., 2004). This strain was shown to belong to A/Arg/01 serotype, and its virulent phenotype could be reproduced in the laboratory in suckling mice as well as in adult animals (García Núñez et al., 2010). Interestingly, upon inoculation of adult mice with FMDV A/Arg/01, two viral variants displaying singular infection patterns were detected. Specifically, 10^5 PFU of each virus were inoculated ip per animal in C57BL/6J/LAE mice, and mice were monitored for signs of disease for 7 days. Signs of disease in animals inoculated with one variant included reduced activity and slower response to external stimuli, which were only apparent and lasted for 2 days. Conversely, infection with the second variant led to severe signs of disease such as ruffled fur, humped posture and tremor, along with a more pronounced decrease in activity and response to stimuli. As shown in Fig. 1A, mice inoculated with the former variant remained alive after 7 days post-

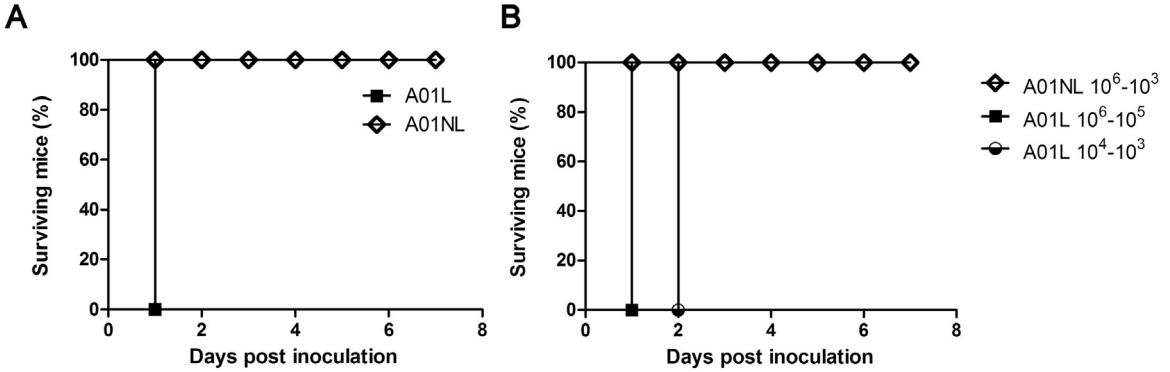

Fig. 1. Survival of C57BL/6/LAE adult mice after inoculation with FMDV variants. (A) Groups of eight to ten week-old mice (n=9) were inoculated intraperitoneally with 10^5 PFU of A01L or A01NL and observed for 7 days. (B) Mice (n=3) were inoculated intraperitoneally with different doses of A01L or A01NL and observed for 7 days. Viral inoculum is indicated in number of PFU per animal.

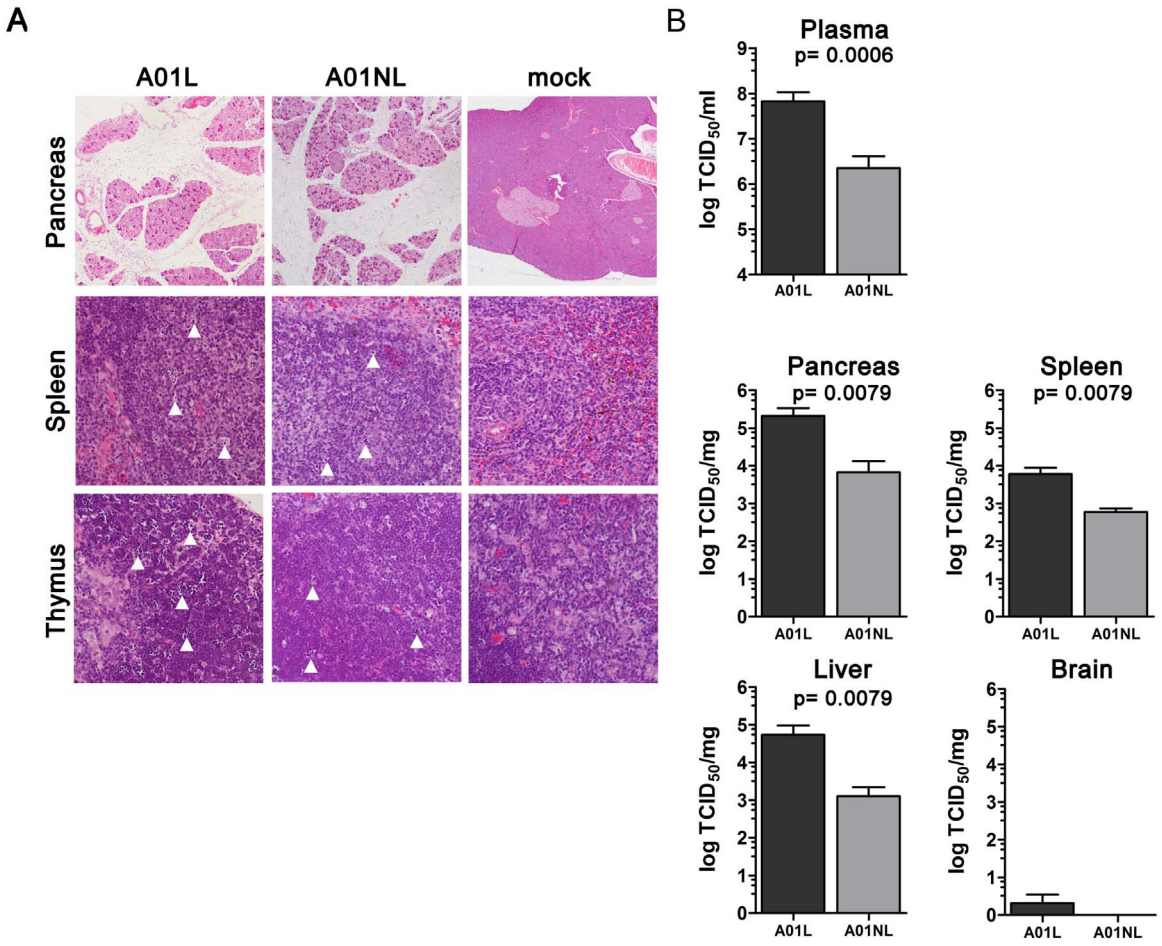

Fig. 2. Pathogenicity of A01L and A01NL infection in adult mice. (A) Tissue sections of pancreas (40X), spleen (200X) and thymus (200X) from inoculated mice. Tissues were harvested at 22 hpi. Hematoxylin and eosin staining are shown. White triangles denote apoptotic cells. (B) Viral titers in plasma (n=9) and tissues (n=5) of inoculated animals at 22 hpi. The bars show mean viral titers and SD for each group; p values (Student's *t*-test) are indicated. Data are representative of two independent experiments.

inoculation (dpi), whereas 100% of animals inoculated with the latter showed irreversible signs of disease or even died at ~24 h post-inoculation (hpi). Thus, viral variants were termed non-lethal (A01NL) or lethal (A01L), respectively, according to the phenotype exhibited in C57BL/6J/LAE mice.

In order to evaluate whether the observed phenotype was dose-dependent, groups of mice were inoculated ip with serial dilutions of A01L and A01NL and monitored for 7 days. As depicted in Fig. 1B, most mice inoculated with A01L died within the first 48 hpi independently of the viral dose used; mice inoculated with A01NL remained alive even at doses as high as 10^6 PFU per animal. These results suggest that lethality of A01L is determined by viral factors independently of the dose used.

Pathological changes in tissues of mice inoculated with 10^5 PFU of FMDV variants were assessed at 22 hpi (Fig. 2A). Severe lesions were evidenced in the exocrine pancreas of mice inoculated with A01L and A01NL, which were characterized by necrosis of 80% and 60% of acinar cells, respectively, along with edema and mild infiltration of polymorphonuclear cells. Multifocal apoptosis was evident in the thymus and apoptotic lymphocytes were present in the spleen of mice inoculated with A01L and A01NL, although to a lesser extent in the latter. Lastly, no lesion was detected in liver, lungs, heart or brain of inoculated animals.

To assess viral distribution in inoculated animals, viral load was determined in plasma and in various tissues at 22 hpi. Mice inoculated with both variants displayed high viral titers in plasma, and viremia was significantly higher in mice inoculated with A01L than in animals inoculated with A01NL (Fig. 2B). Indeed, A01L reached consistently higher titers in plasma than A01NL during the first 22 h of infection, despite displaying a similar replication profile (Supplementary Fig 1). Viral titers in pancreas, liver and spleen were also higher in animals inoculated with A01L than in animals inoculated with A01NL (Fig. 2B). Finally, only A01L could be detected in the brain of inoculated animals, although at a low level. These results demonstrate active viral replication of A01L as well as A01NL viruses in mice.

As mentioned above, mice inoculated with A01NL virus showed mild signs of disease, which became evident after 24 hpi and lasted up to 72 hpi (Supplementary Fig 1). In order to evaluate the course of pancreatitis caused by A01NL infection, groups of mice were euthanized at different times post inoculation and histopathological examination of pancreatic tissue was carried out. Acute pancreatitis developed during the first 22 hpi and progressed subsequently to a chronic inflammation with predominance of mononuclear cells along with a pronounced atrophy of the tissue around 14 dpi (Table 1 and Supplementary Fig 2).

FMDV is highly sensitive to type I interferon both *in vitro* (Chinsangaram et al., 2001) and *in* vivo (Chinsangaram et al., 2003). In fact, the IFN-α response is a main component of the immune response against FMDV that controls viral replication. We hypothesized that the higher viral titers observed in mice inoculated with A01L could be attributed to an impaired induction of the innate immune response in these mice. To test this hypothesis, IFN-α levels in plasma were quantified at different times post inoculation with A01L and A01NL. As depicted in Fig. 3, plasma IFN-α levels displayed a similar profile in mice infected with either virus, increasing soon after inoculation and reaching a peak at 14 hpi. Moreover, no significant differences were detected in IFN-α levels between groups of mice. These results demonstrate an appropriate induction of the innate immune response upon infection with A01L and A01NL viruses.

Table 1
Histopathological course of pancreatitis in mice inoculated with A01NL.

Time after inoculation	PMN infiltrate[a]	MN infiltrate[b]	Edema	Atrophy
14 hpi	++		++	
22 hpi	+++		+++	
72 hpi	+++	+	++	+
7 dpi		++	+	++
14 dpi		+++	+	+++

[a] PMN: polymorphonuclear cells.
[b] MN: mononuclear cells.

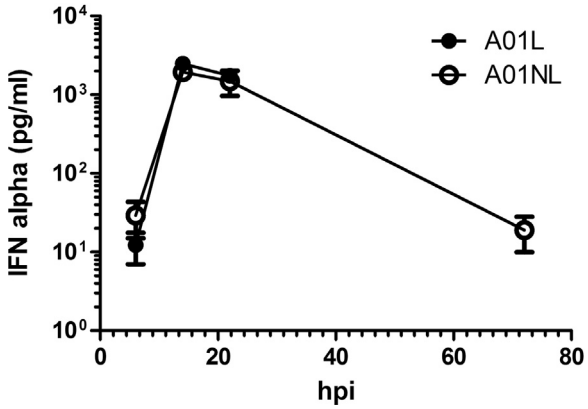

Fig. 3. Quantification of IFN alpha in plasma of inoculated animals at different times post infection. Mean and SD values are shown.

3.2. Cross-protection between FMDV variants

To evaluate whether infection with the non-lethal variant could induce immune protection against A01L infection, groups of mice were inoculated firstly with A01NL virus and 14 days later they received a lethal dose of A01L virus. Mice were monitored for 7 additional days. No animal showed signs of disease during the observation period, while all mice mock-inoculated with DMEM and challenged with A01L died at 48 hpi (Table 2). Circulating neutralizing antibodies were detected in mice inoculated with A01NL and not in mock-inoculated mice prior to inoculation with A01L. Viremia was not detectable at 24 h after A01L inoculation in any A01NL inoculated mouse (Table 2). Thus, infection with A01NL induces neutralizing antibodies that protect adult mice from lethal A01L infection.

3.3. Replication of FMDV variants in cell culture

To assess whether the pathogenicity differences exhibited by A01L and A01NL variants could be reproduced in cell culture, replication of both viruses in cell lines known to support FMDV was evaluated in multiple-step growth curves. No differences became evident in replication profiles of A01L and A01NL variants in IBRS-2, PK15, MDBK or BHK-21 cell lines as well as in bovine fetal kidney cells (BFK). In contrast, significantly different viral titers were detected at 24 and 48 hpi in supernatants of ovine kidney cells (OK) infected with A01L or A01NL, independently of the moi used (Fig. 4A and data not shown).

To further characterize viral replication in cell culture, plaque size and morphology of A01L and A01NL were evaluated at 24 hpi in OK cells. As shown in Fig. 4B, lysis plaques displayed clear morphology in this cell line. Moreover, consistent with our observations in multiple-step growth curves, plaque size of A01L was significantly larger than that of A01NL, further suggesting differential replication kinetics and cytopathogenicity of both viral variants in this cell line. Together, these results indicate particular virus-host interactions driving viral replication in the different cell lines.

Table 2
Protection against lethal infection.

	Inoculation scheme	
	A01NL/A01L	DMEM/A01L
Neutralizing antibody titer[a]	1.69	undetectable
Viremia ($TCID_{50}$/ml)[b]	undetectable	$> 5.6\times10^{7}$
Survival[c] (alive/total mice)	5/5	0/5

[a] Mean antibody titers were determined 14 days after first inoculation and immediately before A01L inoculation.
[b] 1 day after A01L inoculation.
[c] 7 days after A01L inoculation.

3.4. Genomic differences between FMDV variants

In order to assess whether the differential virulence displayed by both FMDV variants could be attributed to genomic changes between them, the complete consensus sequences of A01NL and A01L were determined. Thirty one nucleotide changes were detected along the complete genome between A01NL and A01L. Of them, 25 were located in non-coding regions (n = 2) or turned out to be synonymous changes (n = 23). Additionally, 6 non-synonymous nucleotide changes were detected in VP2 (C2211T and T2515C), VP1 (C3688T and A3775T) and 2C (A4579G and A5086G) coding regions. Non-synonymous changes occurred at non-conserved positions. Of note, these non-synonymous changes were maintained in A01L and A01NL consensus sequences of spleen samples obtained at 22 hpi (Supplementary Table 1).

3.5. Structural analysis of amino acid substitutions in the FMDV capsid

To evaluate the differential influence of amino acid changes on the structure of A01L and A01NL capsids, the four structural proteins were computationally modelled by homology with related X-ray structures and the capsomers assembled by specific computational tools. Mutated positions within VP2 and VP1 proteins were mapped in the three-dimensional model of each viral particle (Fig. 5) and the impact of these mutations on the network of interactions of each residue was analyzed. No relevant effect on protein secondary structure or in their interaction with other residues was predicted for mutations V189A in VP2 and S141L and D170V in VP1. Conversely, the presence of a tyrosine instead of a histidine residue at position 88 of VP2 in A01NL was predicted to originate a more stable interaction with amino acid E218 located at the C-terminus of a second VP2 molecule of the neighboring pentamer. Indeed, residue Y88 proved lower association energy with residue E218 (−2.02 vs −1.77 kcal/mol), which in turn was originated not only by direct Y88 contribution, but also by the invariable residue E218 which presented an improved energy compared with the same E218 residue of A01L (−1.29 vs −1.10 kcal/mol; Supplementary Fig 3). These results suggest increased inter-pentameric association at the 2x axis in A01NL capsids.

We further studied the influence of the capsid mutations on the protonation state and the electrostatic charge of A01L and A01NL capsids across natural pH lowering, namely between pH values 7 and 6, which simulates viral entrance to the early endosomes after receptor recognition. To that end, the electrostatic charge of A01L and A01NL protomers at the 2x axis was calculated and plotted on a structural model of each dimer. As depicted in Fig. 5B, the inter-pentameric interface of A01L dimers showed a progressive and remarkable shift in its predicted protonation state upon decreasing pH values, which is necessary for the establishment of electrostatic repulsion during capsid subunit dissociation. On the contrary, the protonation state of A01NL at the inter-pentameric interface was predicted to remain nearly unchanged between pH 7 and pH 6.5; the interface did not even turn positively charged at pH 6. Thus, A01NL dimers were predicted to be less sensitive from neutral to mildly acidic pH changes.

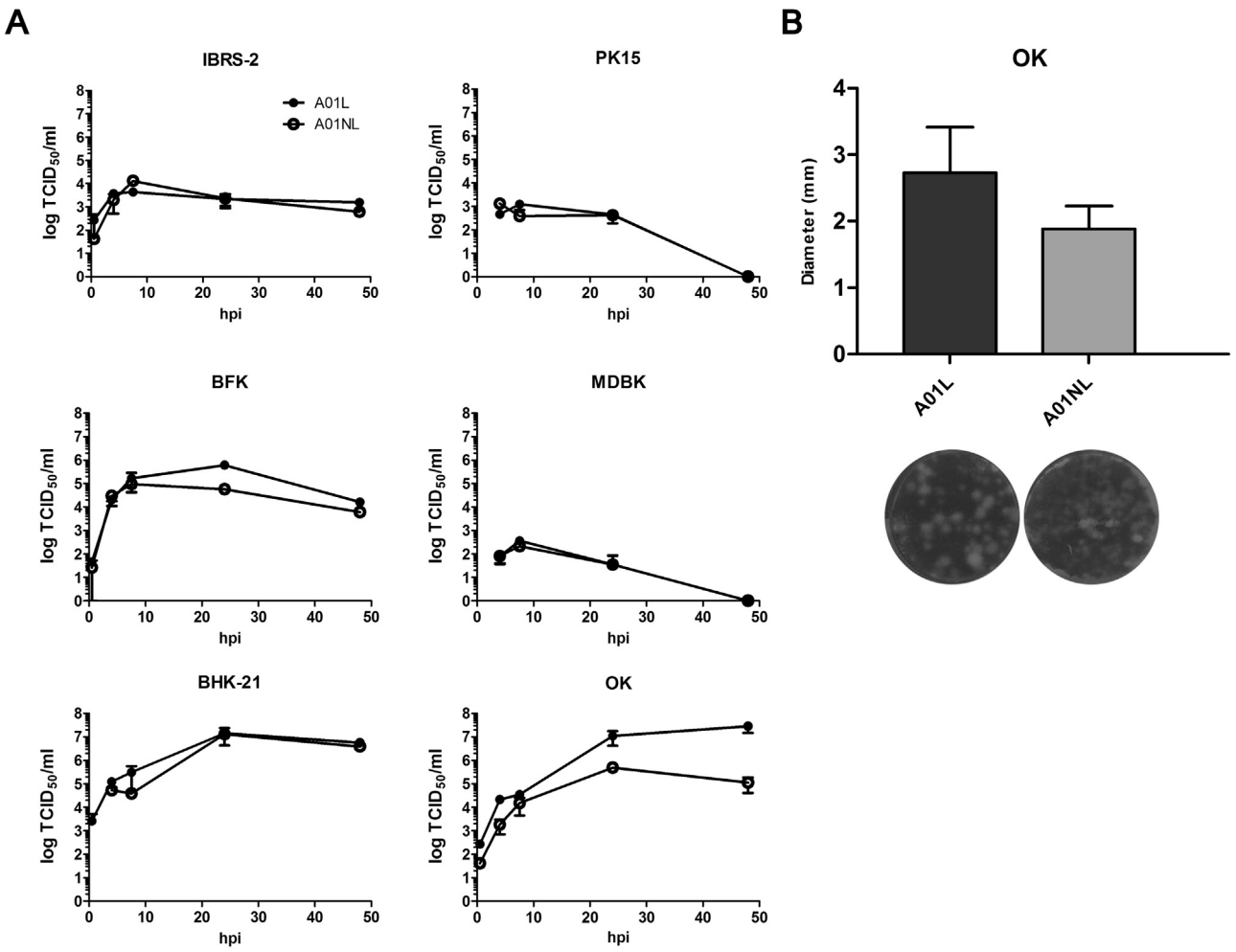

Fig. 4. Replication of FMDV variants in cell culture. (A) Cells were infected with A01L (•) or A01NL (○) with moi=0.1. After adsorption, virus present in supernatants was inactivated by acidification followed by restauration of physiological pH. Virus titration in total cell lysates was performed by end-point dilution in BHK-21 cells. Cell types used are indicated over each plot. Data are representative of at least two independent experiments performed in duplicate. (B) OK cells were infected with A01L and A01NL and plaque diameter was measured at 48 hpi as described in *Material and methods*.

3.6. Analysis of amino acid replacements in 2C protein

FMDV 2C protein is a conserved RNA binding protein with ATPase activity (Sweeney et al., 2010). To predict the impact of amino acid replacements within 2C on protein structure or function, substitutions were mapped in a three-dimensional model of FMDV 2C protein. Amino acid mutations within 2C were located in i) a flexible region between the N-terminal RNA binding domain and the ATPase domain (Q55R) and ii) in the C-terminal portion of the ATPase domain (N224S) (Fig. 6A). However, mutation N224S was not located in ATPase motifs Walker A, Walker B or C (Gorbalenya et al., 1990).

We also analyzed the frequency of these mutations in other FMDV isolates. As shown in Fig. 6B, residue R_{55}, present in A01NL virus, was predicted to be a frequent event within FMDV. In turn, A01L amino acid N_{224} corresponds to a conserved residue within all FMDV serotypes. Of note, A01L residue Q_{55} and A01NL residue S_{224} were not detected in an alignment of 136 FMDV sequences of serotype A (Supplementary Fig 4).

4. Discussion

Since the discovery in 1897 that foot-and-mouth disease was caused by a viral agent (Loeffler and Frosch, 1897), scientific efforts have focused on the development of control measures of this highly devastating disease. The early demonstration that guinea pigs could reproduce FMDV infection in natural hosts provided the means to evaluate experimental vaccines (Waldman and Pape, 1920); it also led to the introduction of other animal models that proved to be useful to study other singular aspects of FMDV infection (Skinner, 1951; Salguero et al., 2005). Although viral-host interactions seem to be different between natural hosts and animal models, the latter have been used extensively to describe viral replication in animals and specifically to evaluate immune responses in a simple way during the development of prophylactic strategies against FMDV. In particular, the adult C57BL/6 mouse model proposed by Salguero et al. allows evaluation of susceptibility and resistance to lethal infection (Salguero et al., 2005), thus becoming particularly useful to characterize FMDV A/Arg/01 strains with subtle genomic differences as the ones analyzed in the present work.

In mice, clinical outcome after FMDV infection has been related to viral serotype and route of inoculation. Indeed, susceptibility of C57BL/6 mice proved to be different to FMDV serotypes C, SAT-1 and A; only 33% of mice inoculated with FMDV A22 died as opposed to 100% of mice inoculated with the other FMDV serotypes (Salguero et al., 2005). Moreover, no signs of disease were detected after exposure of mice to FMDV C-S8c1 by the oronasal route, whereas all animals died within 48–72 h when inoculated subcutaneously in the footpad and even more rapidly when FMDV was inoculated ip (Salguero et al., 2005). In this work, the clinical outcome of inoculated mice was very divergent ranging from a nearly asymptomatic infection

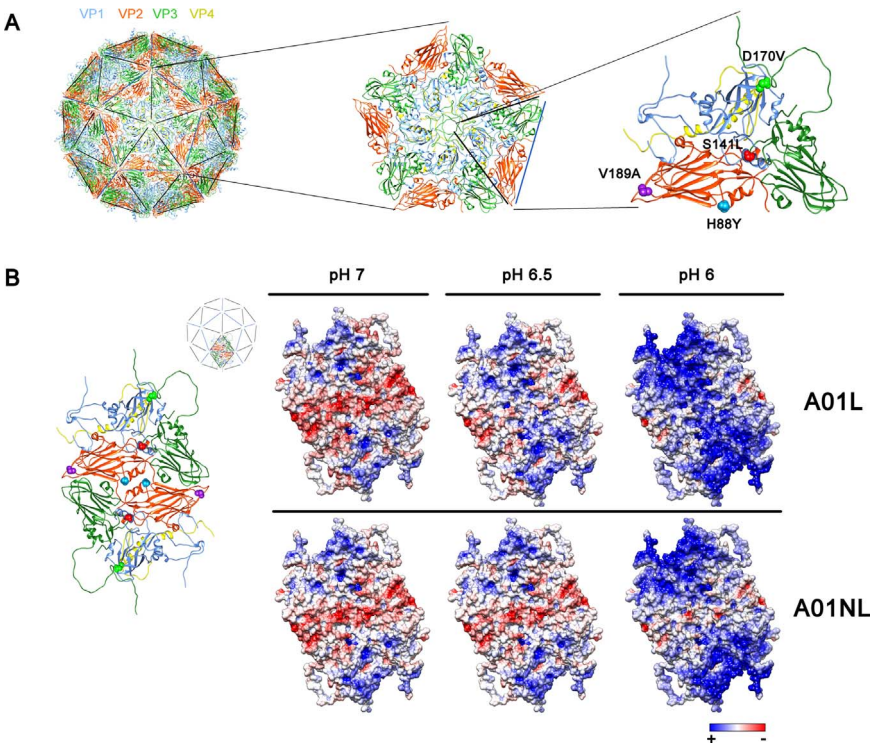

Fig. 5. (A) Homology model of A01L capsid. VP1 is cyan, VP2 is orange, VP3 is green and VP4 is yellow. Amplification of a capsid pentamer and localization of amino acid changes present in A01NL within a single protomer are shown. (B) Analysis of the protonation state of A01L and A01NL dimers on decreasing pH between 7 and 6, as predicted by PROPKA. The structural model of an A01L dimer showing the amino acid substitutions present in A01NL virus is depicted at the left.

to death within 24–48 h. The subcutaneous route of inoculation was not evaluated; however, the differential virulence displayed by both FMDV variants was evidenced using a more stringent way of infection, namely ip inoculation, and the lethal phenotype of A01L persisted even at doses as low as 10^3 PFU/mouse. Interestingly, the dramatic differences in lethality observed for both viruses were not reproduced in cell cultures, where A01NL and A01L viruses showed similar phenotypes. The only exception were OK cells, a cell line derived from ovine kidney that had been shown previously to be more sensitive to FMDV replication than BHK-21 cells (Zabal and Fondevila, 2013). Consequently, OK cells appear as a powerful tool to characterize FMDV isolates with subtle genomic differences as the ones analyzed in this study. Taken together, these results suggest viral-related determinants of virulence and pathogenicity that lead to different virus-host interactions during A01NL and A01L replication in the different biological systems used.

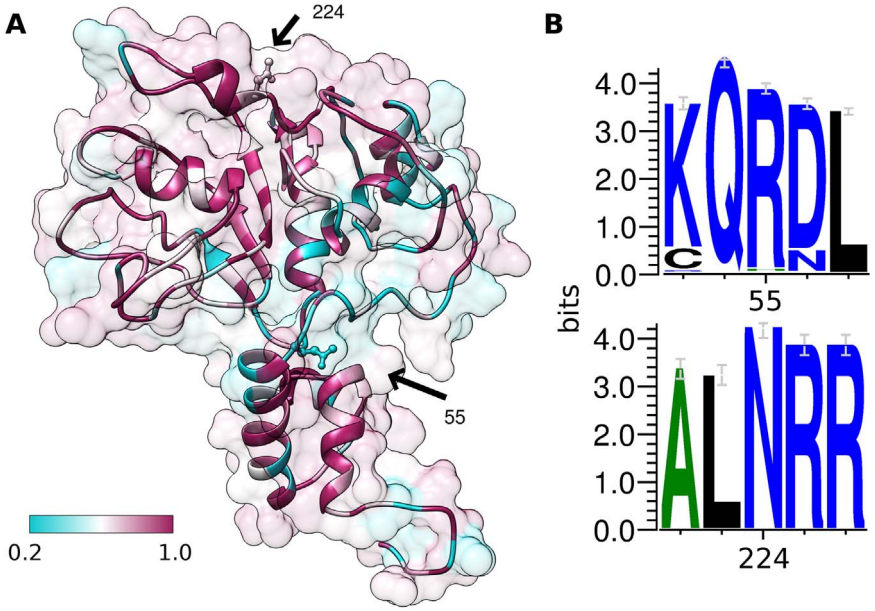

Fig. 6. Analysis of amino acid changes within 2C protein. (A) Homology model of FMDV 2C protein. Black arrows denote mutated residues as indicated. The cyan-maroon key shows the conservation score of each residue as determined from a multiple alignment of 500 FMDV isolates of all serotypes (see *Material and Methods*). (B) Sequence logos showing the conservation of the residues of interest in 500 FMDV sequences of all serotypes. Colors denote hydrophobicity; hydrophilic residues are blue, neutral residues are green and hydrophobic residues are black. Error bars indicate an approximate Bayesian 95% confidence interval.

In this work, adult C57BL/6/LAE mice proved to be adequate to discriminate closely related viruses. A systemic infection occurred in all inoculated mice, as demonstrated by viral distribution in animal tissues independently of the viral variant. However, A01L reached higher levels of viral load than A01NL both in plasma and in organs, and this virus was detected also in the central nervous system, although at low levels. Of note, no microscopic lesions were detected in liver, brain or spleen, suggesting that the virus present in theses tissues mirrors the viremia in each group of animals and does not represent local viral replication. In turn, histopathological observation at 22 hpi revealed that both A01L and A01NL produced necrosis of exocrine pancreatic cells after ip inoculation. Other authors have demonstrated that FMDV infection of adult C57/CE mice causes pancreatic lesions that do not affect the endocrine pancreas and lead even to death within 2–9 days (Platt, 1959). The observations that A01NL also produced severe pancreatic lesions and high viral loads in plasma and tissues deserve particular attention given the only mild clinical signs developed by inoculated animals. These animals controlled viral replication within 72 hpi; however, the acute pancreatic damage evolved to atrophy thereafter. These results are in accordance with previous reports showing viral replication in pancreas that caused a transient or even chronic pancreatitis in different mouse strains (Habiela et al., 2014; Fernández et al., 1986).

A severe but transient lymphopenia has been documented in swine during acute infection with FMDV, which coincides with the viremia peak and in some cases has been related to lymphocyte infection *in vivo* (Bautista et al., 2003; Diaz-San Segundo et al., 2006). Similarly, adult mice showed a decrease in plasma lymphocyte counts and loss of splenic $CD8^+$ lymphocytes and dendritic cells after subcutaneous or ip FMDV inoculation, thus mimicking the transient immunosuppression observed in swine during acute infection (Salguero et al., 2005; Langellotti et al., 2012). However, FMDV infection in mice elicits a T-independent response leading to the early production of high titers of neutralizing antibodies prior to the induction of T-dependent long lasting immunity (Borca et al., 1986). Accordingly, in our work plasma IFN-α levels increased as soon as 6 hpi and reached a peak at 22 hpi both in A01L and A01NL inoculated mice. Furthermore, mice inoculated with A01NL not only controlled infection within a few days but also mounted a protective immune response against A01L efficiently. These results argue in favor of an immunocompetent state in A01L and A01NL infected mice. Interestingly, A01L outperformed A01NL replication levels even in a similar immune context, which reinforces the idea of viral traits implicated in the observed phenotype.

Complete consensus sequences of A01L and A01NL variants revealed a number of substitutions located along the genome. Of them, 2 changes were placed in the 5′ untranslated region, namely at positions 757 and 1033 within the IRES element, which guides translation of the viral genome in a cap-independent manner (Grubman and Baxt, 2004). The structure of the FMDV IRES and its interaction with cellular proteins have been studied widely (Martínez-Salas et al., 2015). In a previous work, we interrogated the structure of the IRES element of A01NL virus using SHAPE (García Núñez et al., 2014). In this early work, positions 757 and 1033 showed no SHAPE reactivity, indicating that they are involved in RNA:RNA interactions. Of note, nucleotide mutations present in A01L virus, which occur in the basal stem of domain 3 (G_{757}→A) and near the A-rich region of domain 4(K) (C_{1033}→U), were not predicted to alter the secondary structure of the IRES element (Supplementary Fig 5), suggesting no effect in IRES translation efficiency between A01NL and A01L variants. So, we decided to concentrate on the six non-synonymous mutations occurring between both variants.

We hypothesized that amino acid changes in VP2 and VP1 proteins could cause differential interactions between A01NL and A01L capsids and the host cell, thus leading to the differential replication observed. It is well known that FMDV may utilize a number of cell receptors for viral entry, including different integrins and heparan sulfate in cell culture (Sa-Carvalho et al., 1997; Neff et al., 1998; Baranowski et al., 2000). Viral attachment to the host cell is followed by receptor recognition through a conserved RGD motif located in the GH loop (Verdaguer et al., 1995; Mason et al., 1994) within VP1 protein. In this work, we found a conserved RGD motif in A01L and A01NL viruses, along with mutation S141L in A01NL variant, which occurred within the GH loop, namely at position RGD −3. Although this amino acid change could somehow affect receptor binding, it has been demonstrated previously that the stability of FMDV binding to cellular integrins depends on the leucine residues located at RGD +1 and +4 positions, which stabilize the VP1-integrin complex thus increasing viral infectivity (Dicara et al., 2008). So, since the RGD motif and both leucine residues are present in A01L and A01NL viruses, we believe that receptor binding of A01NL virus should not be affected. Indeed, *in silico* predicted structural models of both capsids did not show relevant differences, and neutralizing antibodies raised against A01NL blocked replication of A01L within 24 h in mice, meaning that the four amino acid changes present in the capsid region of both viruses do not impair cross-neutralization.

After endocytosis, acidification of endosomes drives capsid disassembly into its pentameric subunits and release of the FMDV genome in the cytoplasm (Baxt, 1987; Carrillo et al., 1985), where RNA translation and replication take place in association with endomembranes (Midgley et al., 2013). Residues located at the interpentameric interface are involved in particle disassembly (Martin-Acebes et al., 2010; Caridi et al., 2015). In fact, mildly acidic pH favors protonation of histidine residues close to the interpentameric interface, leading to electrostatic repulsion between capsid subunits and promoting capsid disassembly. In this work, the electrostatic charge of A01L and A01NL capsids was predicted to differ upon pH lowering, which suggests a differential sensitivity to mildly acidic pH of both viruses. At the same time, we found a histidine to tyrosine mutation in VP2 residue 88, located within the interpentameric interface. This Y residue was predicted to yield a more stable interaction with VP2 residue E218 of the neighboring pentamer, suggesting increased capsid stability of A01NL particles. Strikingly, *in vitro* determination of acid and thermal stability of both viruses produced variable results in independent experiments, with A01L and A01NL variants displaying irregular responses to pH or temperature changes (data not shown). These contrasting results might be related to the quasispecies nature of A01L and A01NL viruses, which could lead to the existence of variants with different sets of amino acid mutations and diverse stability. Additional studies using infectious cDNA clones including different combinations of the four capsid changes are needed to elucidate whether these mutations indeed affect virion stability.

Mutations occurring within 2C-coding region led to amino acid changes Q55R and N224S present in A01NL virus. Interestingly, residue 55 within 2C of a type C FMDV had been related previously to the magnitude of the cytopathic effect elicited by the virus in BHK-21 cells. Specifically, cells infected with a virus bearing an R55W mutation detached more rapidly from the monolayer, thus suggesting a role of residue 55 in virulence (Arias et al., 2010). In turn, A01L residue N224 is a highly conserved amino acid located in the ATPase domain of FMDV 2C protein. The presence of an infrequent residue such as serine at this position might be related to the reduced replication exhibited by A01NL virus in mice.

In sum, we propose that the amino acid mutations found between A01L and A01NL viruses determine the course of viral replication in mice thus contributing to the differential phenotypes observed. Additional studies using mutant viruses in this highly sensitive model are being carried out in order to establish whether lethality is determined by a particular amino acid or rather by a combination of all amino acid substitutions.

Acknowledgments

This work was supported by grants PICT 725–2011 and PICT 982–2014 from Agencia Nacional de Promoción Científica y Tecnológica and Project PNSA 1115052 from Instituto Nacional de Tecnología Agropecuaria (Argentina). M.C. and A.C. are doctoral fellows of the National Research Council (CONICET) at the University of Luján, Argentina, and P.M., M.I.G. and E.C. are members of the CONICET Research Career Program. We thank Osvaldo Zábal, Juan Manuel Schammas and Javier Rosende for technical assistance during our work in the BSL4-OIE facilities at the Institute of Virology–INTA.

Appendix A. Supporting information

Supplementary data associated with this article can be found in the online version at doi:10.1016/j.virol.2017.06.012.

References

Altschul, S.F., et al., 1997. Gapped BLAST and PSI-BLAST: a new generation of protein database search programs. Nucleic Acids Res 25, 3389–3402.
Arias, A., et al., 2010. Deletion mutants of VPg reveal new cytopathology determinants in a picornavirus. PLoS ONE 5 (5), e10735.
Arnold, K., et al., 2006. The SWISS-MODEL workspace: a web-based environment for protein structure homology modelling. Bioinformatics 22 (2), 195–201.
Arzt, J., et al., 2011. The pathogenesis of foot-and-mouth disease I: viral pathways in cattle. Transbound. Emerg. Dis. 58, 291–304.
Baranowski, E., et al., 2000. Cell recognition by foot-and-mouth disease virus that lacks the RGD integrin-binding motif: flexibility in aphthovirus receptor usage. J. Virol. 74 (4), 1641–1647.
Bautista, E.M., Ferman, G.S., Golde, W.T., 2003. Induction of lymphopenia and inhibition of T cell function during acute infection of swine with foot and mouth disease virus (FMDV). Vet. Immunol. Immunopathol. 92 (1–2), 61–73.
Baxt, B., 1987. Effect of lysosomotropic compounds on early events in foot-and-mouth disease virus replication. Virus Res 7 (3), 257–271.
Borca, M.V., et al., 1986. Immune response to foot-and-mouth disease virus in a murine experimental model: effective thymus-independent primary and secondary reaction. Immunology 59 (2), 261–267.
Borca, M.V., et al., 2012. Role of arginine-56 within the structural protein VP3 of foot-and-mouth disease virus (FMDV) O1 Campos in virus virulence. Virology 422, 37–45.
Bøtner, A., et al., 2011. Capsid proteins from field strains of foot-and-mouth disease virus confer a pathogenic phenotype in cattle on an attenuated, cell-culture-adapted virus. J. Gen. Virol. 92, 1141–1151.
Caridi, F., et al., 2015. The pH stability of foot-and-mouth disease virus particles is modulated by residues located at the pentameric interface and in the N terminus of VP1. J. Virol. 89 (10), 5633–5642.
Carrillo, E.C., Giachetti, C., Campos, R.H., 1985. Early steps in FMDV replication: further analysis on the effect of chloroquine. Virology 147, 118–125.
Carrillo-Tripp, M., et al., 2009. VIPERdb2: an enhanced and web API enabled relational database for structural virology. Nucleic Acids Res 37 (Database issue), D436–D442.
Chinsangaram, J., et al., 2003. Novel viral disease control strategy: adenovirus expressing alpha interferon rapidly protects swine from foot-and-mouth disease. J. Virol. 77, 1621–1625.
Chinsangaram, J., Mason, P.W., Grubman, M.J., 1998. Protection of swine by live and inactivated vaccines prepared from a leader proteinase deficient serotype A12 foot-and-mouth disease virus. Vaccine 16, 1516–1522.
Chinsangaram, J., Koster, M., Grubman, M.J., 2001. Inhibition of L-deleted foot-and-mouth disease virus replication by alpha/beta interferon involves double-stranded RNA-dependent protein kinase. J. Virol. 75 (12), 5498–5503.
Crooks, G.E., et al., 2004. WebLogo: a sequence logo generator. Genome Res. 14, 1188–1190.
Diaz-San Segundo, F., et al., 2006. Selective lymphocyte depletion during the early stage of the immune response to foot-and-mouth disease virus infection in swine. J. Virol. 80 (5), 2369–2379.
Díaz-San Segundo, F., et al., 2012. Inoculation of swine with Foot-and-Mouth Disease SAP-mutant virus induces early protection against disease. J. Virol. 86 (3), 1316–1327.
Dicara, D., et al., 2008. Foot-and-mouth disease virus forms a highly stable, EDTA-resistant complex with its principal receptor, integrin alphavbeta6: implications for infectiousness. J. Virol. 82 (3), 1537–1546.
Domingo, E., et al., 2003. Evolution of foot-and-mouth disease virus. Virus Res 91 (1), 47–63.
Domingo, E., Davila, M., Ortin, J., 1980. Nucleotide sequence heterogeneity of the RNA from a natural population of foot-and-mouth-disease virus. Gene 11, 333–346.
Fernández, F.M., et al., 1986. Foot-and-mouth disease virus (FMDV) experimental infection: susceptibility and immune response of adult mice. Vet. Microbiol 12, 15–24.
García Núñez, S., et al., 2010. Differences in the virulence of two strains of foot-and-mouth disease virus serotype A with the same spatiotemporal distribution. Virus Res 147, 149–152.
García Núñez, S., et al., 2014. Enhanced IRES activity by the 3′UTR element determines the virulence of FMDV isolates. Virology 448, 303–313.
Glaser, F., et al., 2003. ConSurf: identification of functional regions in proteins by surface-mapping of phylogenetic information. Bioinformatics 19 (1), 163–164.
Gorbalenya, A.E., Koonin, E.V., Wolf, Y.I., 1990. A new superfamily of putative NTP-binding domains encoded by genomes of small DNA and RNA viruses. FEBS Lett. 262 (1), 145–148.
Grubman, M.J., Baxt, B., 2004. Foot-and-mouth disease. Clin. Microbiol Rev. 17 (2), 465–493.
Habiela, M., et al., 2014. Laboratory animal models to study foot-and-mouth disease: a review with emphasis on natural and vaccine-induced immunity. J. Gen. Virol. 95, 2329–2345.
Haydon, D.T., et al., 2001. Evidence for positive selection in foot-and-mouth disease virus capsid genes from field isolates. Genetics 157, 7–15.
Landau, M., et al., 2005. ConSurf 2005: the projection of evolutionary conservation scores of residues on protein structures. Nucleic Acids Res 33 (Web Server issue), W299–W302.
Langellotti, C., et al., 2012. Foot-and-mouth disease virus causes a decrease in spleen dendritic cells and the early release of IFN-alpha in the plasma of mice. Differences between infectious and inactivated virus. Antivir. Res 94 (1), 62–71.
Lawrence, P., et al., 2016a. Pathogenesis and micro-anatomic characterization of a cell-adapted mutant foot-and-mouth disease virus in cattle: impact of the Jumonji C-domain containing protein 6 (JMJD6) and route of inoculation. Virology 492, 107–117.
Lawrence, P., et al., 2016b. Role of Jumonji C-domain containing protein 6 (JMJD6) in infectivity of foot-and-mouth disease virus. Virology 492, 38–52.
Loeffler, F., Frosch, P., 1897. Summarischer Bericht über die Ergebnisse der Untersuchungen der Kommission zur Erforschung der Maul- und Klauenseuche bei dem Institut für Infektionskranheiten. Dtsch Med Wschr 98, 80–84.
Lohse, L., et al., 2012. Capsid coding sequences of foot-and-mouth disease viruses are determinants of pathogenicity in pigs. Vet. Res 43 (1), 46.
Martin-Acebes, M.A., et al., 2010. A single amino acid substitution in the capsid of foot-and-mouth disease virus can increase acid lability and confer resistance to acid-dependent uncoating inhibition. J. Virol. 84 (6), 2902–2912.
Martínez-Salas, E., et al., 2015. Picornavirus IRES elements: RNA structure and host protein interactions. Virus Res. 206, 62–73.
Mason, P.W., et al., 1997. Evaluation of a live-attenuated foot-and-mouth disease virus as a vaccine candidate. Virology 227, 96–102.
Mason, P.W., Rieder, E., Baxt, B., 1994. RGD sequence of foot-and-mouth disease virus is essential for infecting cells via the natural receptor but can be bypassed by an antibody-dependent enhancement pathway. Proc. Natl. Acad. Sci. USA 91, 1932–1936.
Mattion, N., et al., 2004. Reintroduction of foot-and-mouth disease in Argentina: characterisation of the isolates and development of tools for the control and eradication of the disease. Vaccine 22, 4149–4162.
McGuffin, L.J., et al., 2015. IntFOLD: an integrated server for modelling protein structures and functions from amino acid sequences. Nucleic Acids Res 43 (W1), W169–W173.
Midgley, R., et al., 2013. A role for endoplasmic reticulum exit sites in foot-and-mouth disease virus infection. J. Gen. Virol. 94 (Pt 12), 2636–2646.
Molinari, P., et al., 2010. Baculovirus treatment fully protects mice against a lethal challenge of FMDV. Antivir. Res 87 (2), 276–279.
Neff, S., et al., 1998. Foot-and-mouth disease virus virulent for cattle utilizes the integrin alpha(v)beta3 as its receptor. J. Virol. 72 (5), 3587–3594.
Núñez, J.I., et al., 2001. A single amino acid substitution in non-structural protein 3A can mediate adaptation of foot-and-mouth disease virus to the guinea pig. J. Virol. 75, 3977–3983.
Pacheco, J.M., et al., 2013. A partial deletion in non-structural protein 3A can attenuate foot-and-mouth disease virus in cattle. Virology 446, 260–267.
Papadopoulos, J.S., Agarwala, R., 2007. COBALT: constraint-based alignment tool for multiple protein sequences. Bioinformatics 23, 1073–1079.
Pettersen, E.F., et al., 2004. Chimera-a visualization system for exploratory research and analysis. J. Comput. Chem. 25 (13), 1605–1612.
Platt, H., 1959. The occurrence of pancreatic lesions in adult mice infected with the virus of foot-and-mouth disease. Virology 9, 484–486.
Quattrocchi, V., et al., 2011. Role of macrophages in early protective immune responses induced by two vaccines against foot and mouth disease. Antivir. Res 92, 262–270.
Reed, L.J., Muench, H., 1938. A simple method of estimating fifty percent endpoints. Am. J. Hyg. 27, 493–497.
Rieder, E., et al., 1996. Propagation of an attenuated virus by design: engineering a novel receptor for a noninfectious foot-and-mouth disease virus. Proc. Natl. Acad. Sci. USA 93 (19), 10428–10433.
Sa-Carvalho, D., et al., 1997. Tissue culture adaptation of foot-and-mouth disease virus selects viruses that bind to heparin and are attenuated in cattle. J. Virol. 71 (7), 5115–5123.
Salguero, F.J., et al., 2005. Foot-and-mouth disease virus (FMDV) causes an acute disease that can be lethal for adult laboratory mice. Virology 332, 384–396.
Schneider, C.A., Rasband, W.S., Eliceiri, K.W., 2012. NIH Image to ImageJ: 25 years of image analysis. Nat. Methods 9 (7), 671–675.
Schneider, T.D., Stephens, R.M., 1990. Sequence logos: a new way to display consensus sequences. Nucleic Acids Res 18, 6097–6100.
Skinner, H.H., 1951. Propagation of strains of foot-and-mouth disease virus in unweaned white mice. Proc. R. Soc. Med 44, 1041–1044.
Sobrino, F., et al., 1983. Multiple genetic variants arise in the course of replication of foot-and-mouth disease virus in cell culture. Virology 128, 310–318.

Sobrino, F.D., Domingo, E., 2004. Foot-and-Mouth Disease. Horizon Press, London.
Sweeney, T.R., et al., 2010. Foot-and-mouth disease virus 2C is a hexameric AAA+ protein with a coordinated ATP hydrolysis mechanism. J. Biol. Chem. 285 (32), 24347–24359.
Verdaguer, N., et al., 1995. Structure of the major antigenic loop of foot-and-mouth disease virus complexed with a neutralizing antibody: direct involvement of the Arg-Gly-Asp motif in the interaction. EMBO J. 14, 1690–1696.
Waldman, O., Pape, J., 1920. Die künstliche Übertragung der Maul- und Klauenseuche auf das Meerschweinchen. Berl. Munch. Tierarztl. Wochenschr. 36, 519–520.
Zabal, O., Fondevila, N., 2013. Selection of highly susceptible cell lines to foot and mouth disease virus infection. Open J. Vet. Med 3, 263–266.
Zhao, Q., Pacheco, J.M., Mason, P.W., 2003. Evaluation of genetically engineered derivatives of a Chinese strain of foot-and-mouth disease virus reveals a novel cell-binding site which functions in cell culture and in animals. J. Virol. 77 (5), 3269–3280.
Zuker, M., 2003. Mfold web server for nucleic acid folding and hybridization prediction. Nucleic Acids Res. 31, 3406–3415.